Clay Minerals (2023), **57**, 202–210
doi:10.1180/clm.2022.38

CAMBRIDGE UNIVERSITY PRESS

Article

Muttalip green clay and its ultraviolet and infrared absorption and reflection

Hülya Kuru Mutlu*
Eskisehir Osmangazi University, Vocational School of Health Services, Opticianry Program, 26040, Eskisehir, Turkey

Abstract

The search for sufficiently high-quality clays for use in the tile industry represents a significant challenge. This study aimed to prepare Muttalip green clay tiles with flexural strengths adhering to the TS EN 1304:2016 standard. Muttalip green clay was subjected to sieving, vacuum pressed, dried and then baked to obtain galette tiles. The tiles were analysed subsequently using optical techniques, including X-ray diffraction, X-ray fluorescence spectrometry and field-emission scanning electron microscopy. The influence of various firing temperatures (900, 950 and 1000°C) on the flexural strength of the tiles was also investigated. The tiles obtained at 950°C exhibited a maximum flexural strength of 153.91 kg cm^{-2}. Fourier-transform infrared spectroscopy revealed that the tiles reflect ultraviolet A radiation and absorb infrared radiation. Muttalip green clay is a suitable material for preparing tiles for roofing applications.

Keywords: FE-SEM, flexural strength, FTIR, green clay, Muttalip, optical characterization

(Received 28 June 2022; revised 28 November 2022; Accepted Manuscript online: 9 December 2022; Associate Editor: D. Bish)

The construction industry is vital for the global economy because of the goods and services it produces (Assuncao *et al.*, 2021; Da Costa *et al.*, 2021). Tiles are used to construct roof structures because they are natural, insulating and lightweight; thus, they offer essential protection to buildings. However, a sustainable resource for the clay used in tile production needs to be developed.

Clay, the basic material used to produce roof tiles, plays an important role in meeting the requirements of a growing consumer market (Lee & Yeh, 2008). Site-specific materials are very important in the construction industry. To encourage the development and importing of such materials, the support of the construction industry is needed. Although the value of these topics has been emphasized, progress in the construction industry regarding such matters in developing countries remains limited (Ofori, 2019).

Insufficient reserves and low-quality clay are challenges that affect tile production. Knowledge of the chemical properties and sieve analysis results of clays is important for tile production. Clays undergo various reactions in the crusher during tile production depending on their structure before a final product can be obtained (Turkish Republic Prime Ministry State Planning Organization, 2008).

The suitability of a clay for use in tile production depends on its mineralogy and the amount and types of impurities it contains. The physical properties of the materials obtained from clays, such as their drying shrinkage, firing shrinkage, water absorption and flexural strength, must be measured before tile production. Selecting a proper raw material is crucial for obtaining the desired product. Clay analysis reduces product losses by minimizing and simplifying the necessary interventions during production (Vieira *et al.*, 2008).

Due to the lack of productive clay deposits in many countries, only a few studies on the use of clays as raw materials for tile production have been reported (Piskin & Figen, 2013; Sultana *et al.*, 2015; De Silva & Mallwattha, 2017, 2018; Assuncao *et al.*, 2021; Simao *et al.*, 2021). In this study, Muttalip green clay with flexural strength adhering to the TS EN 1304:2016 quality standard was prepared and characterized. Firing was performed at various temperatures to improve the flexural strength of the tiles. The water absorption of the tiles obtained was measured and their absorptive and reflective properties in the ultraviolet (UV) and infrared (IR) regions were investigated. Roof-tile production analyses were performed at the research and development laboratory of Hatipoglu Günes Tile & Brick Industry, Inc. (Turkey). This study contributes to the literature by detailing the industrial production and optical analysis of this clay.

Materials and methods

Study area

The green clay used in this study was obtained from Muttalip, Eskişehir Province, Turkey. The study area was located using a GPS map (60CSx) at 39°51′35.3″N, 30°30′56.5″E.

The green clay field is located in Muttalip (Fig. 1), where open quarries and a thin cover layer of brick tile clay are present. Quaternary-aged alluvial, terrestrial and sedimentary rock formations are present in the area. Triassic schist and metamorphic rock formations are present at the edges of the area. Mineralization, with an average width and length of 290 and 360 m, respectively, and ore thickness of ~5 m can be observed in the visible reserve area of the field.

*Email: hkuru@ogu.edu.tr
Cite this article: Kuru Mutlu H (2023). Muttalip green clay and its ultraviolet and infrared absorption and reflection. *Clay Minerals* **57**, 202–210. https://doi.org/10.1180/clm.2022.38

Fig. 1. Topographical map of green clay reserves in Muttalip, Eskisehir Province, Turkey. The study area was located using a GPS map (60CSx) at 39°51′35.3′′N, 30°30′56.5′′E, as highlighted in the figure.

Table 1. Particle-size distributions of Muttalip green clay.

Particle size (d, mm)	Muttalip green clay residue (%)
$2 < d < 4$	0.00
$1 < d < 2$	0.00
$0.05 < d < 1$	18.71
$0.025 < d < 0.05$	20.63
$0.0125 < d < 0.025$	20.42
$0.0062 < d < 0.0125$	22.97
$d < 0.0062$	17.27

The green clay was ground using jaw and roller crushers, dried in the shade in an open area and passed through various sieves (*i.e.* 4, 2 and 1 mm and 500, 250, 125 and 63 μm) to determine its particle-size distribution (Table 1), as specified in ASTM C136 (2019). Knowledge of the particle-size distribution of a sample is necessary to assess its properties, such as flexural strength and chemical reactivity, during drying and firing (Milošević *et al.*, 2019, 2020). Clays with dimensions of <1 mm were used as raw materials for tile preparation. Compared with the findings of Akçin *et al.* (2022), the percentage of particles with an average size <25 μm, comprising 60.66% of the green clay material, was lower in this study.

The particle-size distribution of the Muttalip green clay was confirmed using field-emission scanning electron microscopy (FE-SEM; Regulus 8230, Hitachi, Japan). The measurements were obtained at an accelerating voltage of 3 kV, a working distance of 19.6 mm, a low scanning rate and various magnifications (150×, 600×, 100,000×).

Measurements

Mineralogical analysis of the clay was performed using X-ray diffraction (XRD; Empyrean, Malvern Panalytical, UK). The measurements were performed in the 5–90°2θ range, and the spectral peaks obtained were characterized on the basis of the XRD trace (Fig. 2).

The clay components and oxides were measured using X-ray fluorescence (XRF) spectroscopy (Axios Max, Malvern Panalytical). XRF analysis was performed under vacuum, and the results were confirmed using three different measurements with a Rh target tube and 8.0 mm collimator. The parameters of the three measurements were as follows: (1) tube voltage of 15 kV with a 500 μA tube current without a filter; (2) tube voltage of 30 kV with a 1000 μA tube current and a Pb filter; and (3) tube voltage of 15 kV with a 1000 μA tube current and a Cr filter. Loss on ignition (LOI) was determined by heating the sample from 0 to 1050°C for 3.5 h and maintaining it at 1050°C for 30 min. The temperature was then decreased to 24°C by air-cooling for ∼12 h.

The sieved green clay was mixed with water to determine its moisture level, which was measured using a moisture analyser (HB43, Mettler Toledo, OH, USA) after 1 day. The clay was then pressed using a vacuum press device (Sermak Makina, Turkey) to obtain galette tiles. The air-vented galette tiles were dried in an oven (Ref-San, Ceramic Kilns Industry, Turkey) at 80°C, and those exhibiting cracking, breaking and/or discolouration after drying were examined. The dry tiles were fired at various temperatures (900, 950 and 1000°C) in an electric furnace (Ref-San), and the effects of these temperatures on tile flexural strength were investigated. Cracked, broken and discoloured fired tiles were also analysed. The water-holding capacity of the fired tiles was measured to determine their water absorption rate (W_a). A flexural strength test (Kalite Material Testing Equipment Co. Ltd, Turkey) was performed to determine whether the fired tiles exhibited flexural strengths conforming to the TS EN 1304:2016 standard.

The tiles were characterized using Fourier-transform infrared (FTIR) spectroscopy (Bruker Vertex 80v, Nanoboyut Research Laboratory, Turkey). A Globar–SiC 1100°C lamp, a KBr/DLaTGS D301 detector operated at 24°C and a KBr beam splitter were employed for optical measurements in the mid-wave IR (MWIR), long-wave IR (LWIR) and far-IR (FIR) regions. For optical measurements in the near-IR (NIR; 1.00–2.85 μm) region, background and sample measurements were obtained using a tungsten lamp, an indium gallium arsenide (InGaAs) detector and a Ge–CaF_2 beam splitter. The measurements were obtained under vacuum to ensure accuracy between 2.5 and 25.0 μm.

Results and discussion

XRD analysis

The XRD results indicate that Muttalip green clay is composed of SiO_2, albite (Ab), plombièrite (Plm) and muscovite (Ms) $2M_1$ (Fig. 2). SiO_2 is present in ∼95% of the materials used in the

https://doi.org/10.1180/clm.2022.38 Published online by Cambridge University Press

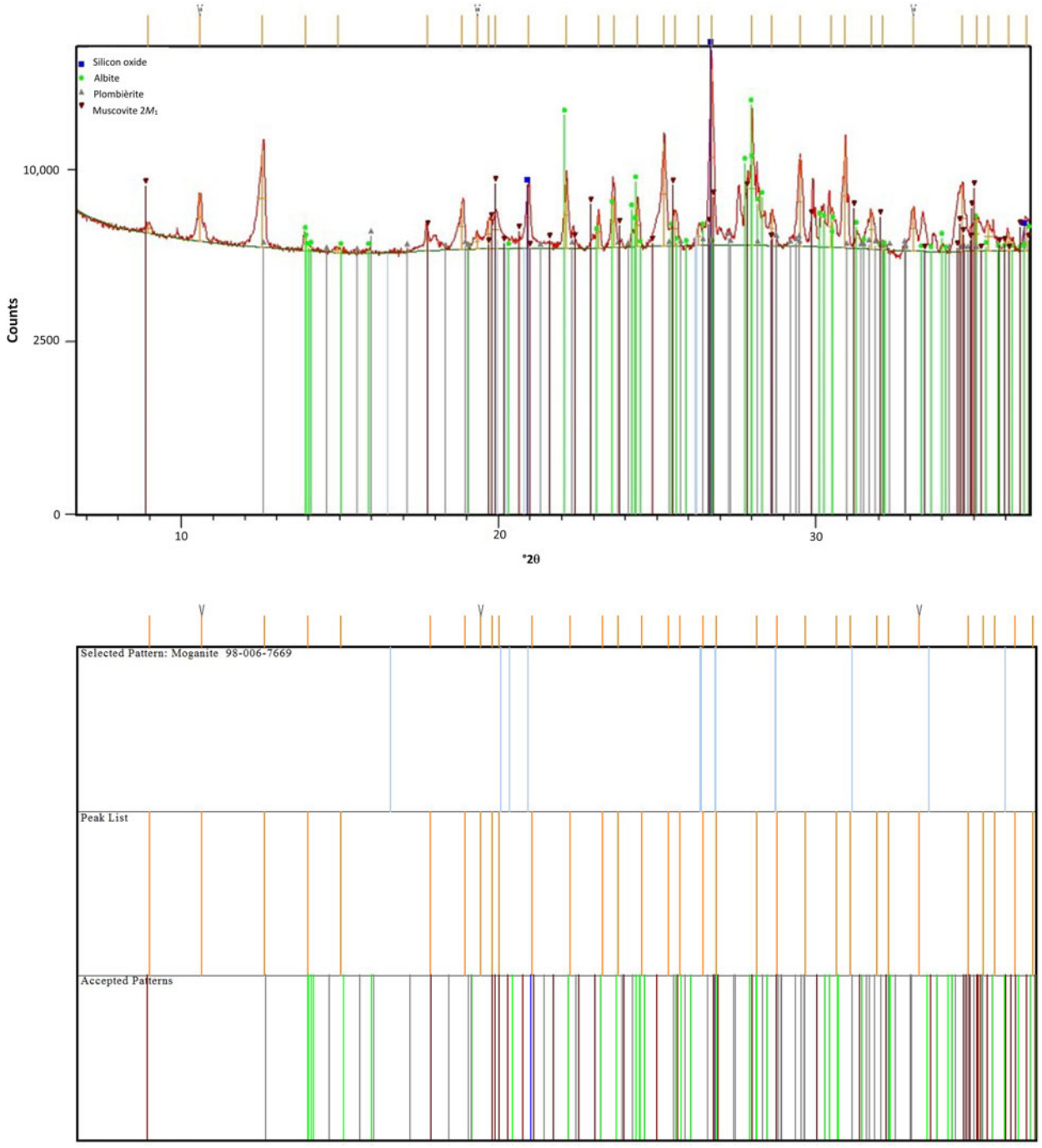

Fig. 2. XRD traces of minerals detected in Muttalip green clay.

construction industry. Nayak & Singh (2007) characterized the clay in their study and determined that quartz (Qz) was the main dense component.

Pure Ab ($NaAlSi_3O_8$) can be white, greenish or reddish, and it is often combined with minerals such as Ms, biotite (Bt), hornblende (Hbl) and Qz. As a precious stone, Ab is used in industries such as glass and ceramic production. Ms is a hydrated phyllosilicate Al- and K-based mineral with the formula $KF_2(Al_2O_3)_3(SiO_2)_6H_2O$ or $KAl_2AlSi_3O_{10}(F,OH)_2$. It can be colourless, greenish, yellowish or reddish. Ms possesses significant Al contents and is employed as a lubricant in the manufacture of non-combustible and insulating materials. In addition to being lightweight, Ms exhibits good flexibility, reflectivity, inertness, dielectric properties, elasticity, hydrophilicity and refractivity (Yuan *et al.*, 2018). It is stable when exposed to electricity, light, humidity and extreme temperatures. Because of all of these features, Ms has been applied widely in various industries. There are also studies in which Ms has been synthesized from an ash

https://doi.org/10.1180/clm.2022.38 Published online by Cambridge University Press

Table 2. Chemical composition (wt.%) of Muttalip green clay.

Oxides	SiO_2	Al_2O_3	Fe_2O_3	TiO_2	CaO	MgO	Na_2O	K_2O	SO_3	LOI1
Mass	34.45	9.16	10.97	2.60	9.42	0.00	0.06	0.65	0.03	32.67

1LOI at 1050°C.

produced from biotite-rich coal wastes (*e.g.* Khoshdast *et al.*, 2021), increasing the availability of this important industrial material. Plm has the formula $(Ca_4Si_6O_{16}(OH)_2{\cdot}2H_2O){\cdot}(Ca{\cdot}5H_2O)$.

XRF measurements

XRF spectroscopy was performed on the Muttalip green clay (Table 2) and it was shown to contain SiO_2, Al_2O_3, Fe_2O_3, TiO_2, CaO, MgO, Na_2O, K_2O and SO_3. SiO_2 and Al_2O_3 as the main components. The large SiO_2 content of the sample confirmed the presence of Qz, as indicated by the XRD results (Fig. 2).

The CaO in the clay indicates the presence of calcite (Cal), as reported by Coletti *et al.* (2016). Cal ($CaCO_3$) often contains small amounts of Fe, small levels of contamination by clay particles and Qz (Milošević *et al.*, 2020). Residual Cal is converted to waste during roof-tile firing, which produces more open pores in these tiles (Montero *et al.*, 2009), leading to increased water absorption (Jordán *et al.*, 2005). The organic matter in the clay may be eliminated using thermal treatment, which also increases the open porosity of the tile (Jordán *et al.*, 2005; De Silva & Mallwattha, 2018). During firing, CaO expands in the ceramic material, leading to the formation of cracks in the tiles. Depending on the reactions that occur at the firing temperature, these cracks can reduce the flexural strength of the material (Assunção *et al.*, 2021).

XRF analysis of the Muttalip green clay revealed a significant amount of CaO in the clay structure. CaO expanded in the tile during firing and decreased its flexural strength; however, when the firing temperature was increased from 900 to 950°C, CaO reacted with amorphous SiO_2 and increased the flexural strength of the tile. When the firing temperature was further increased, CaO decreased the flexural strength of the tile by promoting stress concentration.

LOI enables volatiles to escape from the tiles at high temperatures until their mass stabilizes. The high value of LOI obtained in this study may be attributed to the loss of volatiles, including water (hydrates and unstable hydroxy compounds), organic materials and carbonates (Milheiro *et al.*, 2005; Abdelmalek *et al.*, 2017; Milošević *et al.*, 2020).

The chemical analysis results of the Muttalip green clay were compared with those of other clays used in tile production (Bilgin *et al.*, 2008; Rivera *et al.*, 2018; Moreno-Maroto *et al.*, 2020; Akçin *et al.*, 2022). Among the clays investigated, the Muttalip green clay exhibited the smallest SiO_2 and largest LOI values.

FE-SEM measurements

FE-SEM images of the Muttalip green clay were obtained at various magnifications to analyse its composition and surface morphology. The FE-SEM image obtained at 150× magnification (Fig. 3a) shows particles ranging in size from 30 to 240 µm with an irregular morphology. In a study of tile production using all of the waste from glass bottles, fluorescent lamps and soda-lime window glass, Rivera *et al.* (2018) found smooth, flat-faced and elongated particles; the authors did not observe spherical particles. At 600× magnification (Fig. 3b), smaller clay particles were observed. Small structural cracks were clearly visible at 100,000× magnification (Fig. 3c). Pitarch *et al.* (2021) found that the FE-SEM morphologies of various ground ceramic particles depended on their water absorption. These small variations in morphology are important because tile ceramic particles exhibit

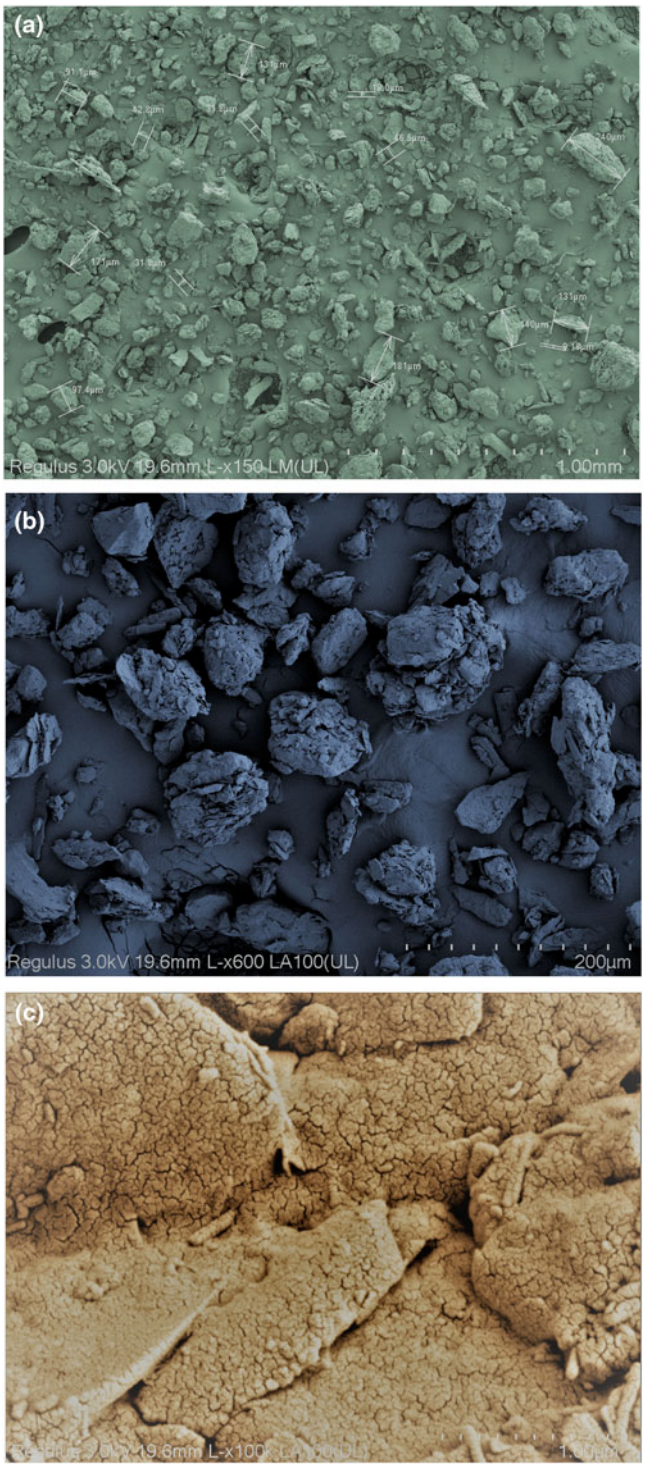

Fig. 3. FE-SEM images of Muttalip green clay at various magnifications.

https://doi.org/10.1180/clm.2022.38 Published online by Cambridge University Press

Table 3. Physical measurements of the galette tiles after drying and firing.

		Sample 1	Sample 2	Sample 3
Wet	Length (mm)	149.08	140.20	110.00
	Width (mm)	51.20	50.60	50.87
	Weight (g)	288.30	268.00	209.80
After drying	Length (mm)	147.00	137.83	107.74
	Width (mm)	48.91	48.53	49.25
	Weight (g)	243.20	226.0	176.90
After firing	Length (mm)	146.26	137.00	107.08
	Width (mm)	48.56	48.20	48.53
	Weight (g)	224.40	207.70	162.50

low porosity and a smooth surface. A small number of small pores could increase the flexural strength of the resulting tile. The FE-SEM images of ceramic materials obtained after sintering at high temperatures (Ahmed *et al.*, 2021) indicated that glassy phase formation and pores could decrease the flexural strength of tile samples.

Moisture rate

Clays present as powders in the absence of water. Thus, a suitable amount of water should be added to a clay to achieve the desired plasticity because water facilitates the weak electrostatic forces necessary for clay–particle attraction (Barnes, 2013). The moisture rate of the Muttalip green clay was 18.25%.

Drying shrinkage

The Muttalip green clay and water were mixed at a humidity level of 15–20% and then poured into a vacuum press to prepare 0.05 × 0.10 m^2 galette tiles containing no air bubbles. The galette tiles were removed from the vacuum press and dried in an oven at 80°C for ~6 h. When the drying temperature was >80°C, the tiles developed cracks, leading to product loss. When the temperature was <80°C, the drying process lasted significantly longer. The width, length and weight of wet (W) and dry (W_d) galette tiles were measured (Table 3) and surface images of the tiles after drying were obtained (Fig. 4). No cracks or breaks were observed in the galette tiles. The surfaces of tiles must be defect-free to achieve a product with good flexural strength. Cracks were observed on the surfaces of galette tiles obtained from Muttalip red clays (Kuru Mutlu, 2022), which exhibited a high SiO_2 content and were dried at 80°C. However, cracks were absent in galette tiles obtained from schist materials (Kuru Mutlu & Mutlu, 2022), which also exhibited a high SiO_2 content and were dried at 80°C. Thus, cracking is not related strongly to the SiO_2 content of the sample.

The masses of the galette tiles before and after drying were compared, and their drying shrinkage values were calculated according to Equation 1 (Table 4; Huggett, 2015). In this study, the drying and weight shrinkage values of the tiles were obtained and referred to collectively as the 'drying shrinkage'. The tiles exhibited a drying shrinkage value that was only 0.45% greater than that of similar tile materials (Kuru Mutlu & Mutlu, 2022); this difference is not significant.

$$\text{Drying shrinkage} = \frac{W - W_d}{W} \times 100\% \quad (1)$$

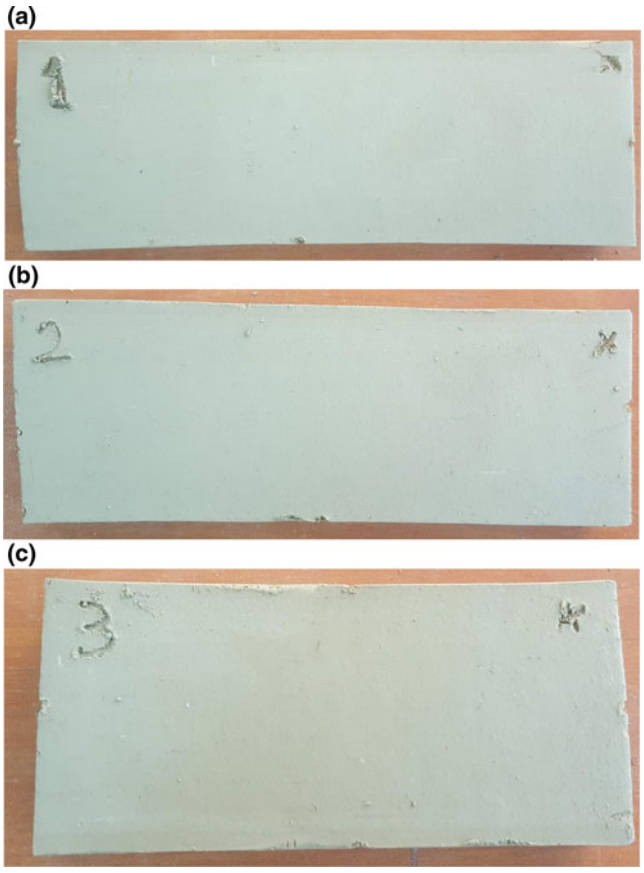

Fig. 4. Images of the galette tiles after drying and heating at 80°C: (a) galette sample 1, (b) galette sample 2 and (c) galette sample 3.

Firing shrinkage

The surfaces of the galettes were defect-free after drying at 80°C. Heat treatment was performed at 900°C (Sample 1), 950°C (Sample 2) and 1000°C (Sample 3) to examine the effects of various firing temperatures on the flexural strength of the tiles. The galette tiles were not removed immediately after firing; instead, the following process was used: the galettes were first heated to 80°C and then rested. Next, they were heated to 473°C and then rested for 1 h. Each sample was then heated to 900, 950 or 1000°C and maintained at this temperature for 2 h. Finally, the galettes were left to air-cool to room temperature.

The width, length and weight (W_f; Table 3) and surface images (Fig. 5) of the fired galette tiles were obtained. None of the tiles showed cracks or fractures because they all contained a small amount of Qz, which serves as a stress concentrator and forms microcracks due to its allotropic transformation (Barnes, 2013). Furthermore, CaO reacts with amorphous SiO_2 to form $CaSiO_3$ during firing and so prevents crack formation as a stress intensifier (Assunção *et al.*, 2021).

All of the ceramics exhibited the reddish colour (Babisk *et al.*, 2020) typical of traditional ceramic products (Fig. 5) due to the oxidation of Fe compounds present in the green clay. Knowledge of the drying and firing shrinkage values of tiles (Equation 2) is important. If desired, the drying and firing shrinkage values can be calculated for each galette using the values from Table 3. Unfortunately, because the firing temperatures of the galettes were different, their average firing shrinkage could not be

https://doi.org/10.1180/clm.2022.38 Published online by Cambridge University Press

Table 4. Average drying shrinkage of the galette tiles.

Physical measurement	Value
Length (%)	1.71
Width (%)	3.91
Weight (%)	15.66

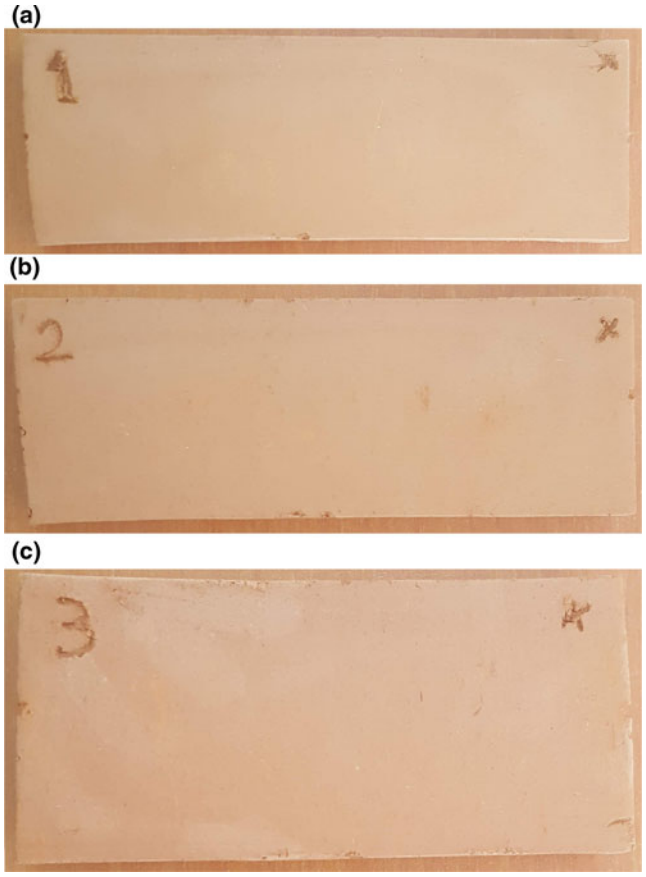

Fig. 5. Images of the galette tiles fired at (a) 900°C, (b) 950°C and (c) 1000°C.

calculated.

$$\text{Firing shrinkage} = \frac{W_d - W_f}{W_d} \times 100\% \quad (2)$$

Water absorption

A dry galette was weighed (W_d) and immersed in water for 24 h. The weight of the tile was then measured after immersion (W_w). Finally, the water absorption (W_a; Equation 3) of the tile was determined (Bureau of Indian Standards, 2002; ASTM C1492, 2003; ASTM C830-00, 2016; De Silva & Mallwattha, 2017). The average W_a of the Muttalip green clay was calculated to be 16.35%.

$$W_a = \frac{W_w - W_d}{W_w} \times 100\% \quad (3)$$

When tiles exhibit significant water impermeability, small plants and algae may grow on them, thereby decreasing their durability and aesthetic values. The water-holding capacity of clay mixtures should not exceed 18% (De Silva & Mallwattha, 2017). The water impermeability of the Muttalip green clay complied with the water-holding capacity limit (18%) of clay roof tiles (Bureau of Indian Standards, 2002; De Silva & Mallwattha, 2017).

Table 5. Flexural strength and converted flexural strength values of galette tiles at various firing temperatures.

	Temperature (°C)		
	900	950	1000
Flexural strength (kg cm^{-2})	64.27	66.92	63.44
Converted flexural strength (kg cm^{-2})	147.82	153.91	145.91

Flexural strength

The most important parameter of a tile is its flexural strength. The breaking flexural strength of the tiles was determined by the maximum load they could withstand using a three-point bending test. Here, the tile was fixed at both ends and various forces were applied at the midpoints of these ends. Then, the breaking flexural strength of each tile was measured using a sensor (Table 5). The effects of various firing temperatures on the flexural strength of the samples were also investigated. The strengths of the galette tiles fired at 900 and 1000°C were similar. Compared with these tiles, the galette fired at 950°C demonstrated increased flexural strength. Specifically, the strength of the galette tile fired at 950°C was 4.12% greater than that of the galette tile fired at 900°C.

In this study, the applicability of de-aerated rectangular galette tiles as roof tiles was investigated. Galette tiles are usually flat. Because Marseille-style tiles, which are frequently used on house roofs, vary in size and shape, a conversion coefficient is required to obtain accurate strength values. A factory production setting is obtained by multiplying the strength value of the Marseille-style tile produced in the laboratory by the factory conversion factor. Tile manufacturers use unique conversion coefficients for laboratory samples (rectangular galettes) and tile production. Thus, the flexural strength of the Muttalip green clay was determined according to the conversion coefficient of Hatipoglu Günes Tile & Brick Industry, Inc. (Table 5). According to the TS EN 1304:2016 and EN ISO 10545-4:2014 standards in Turkey, the breaking load of fired tiles should be >120 kg cm^{-2}. The Muttalip green clay tiles prepared in this study met this standard.

Guimarães *et al.* (2022) reported red clays with flexural strengths of 10.19–91.00 kg cm^{-2}, while Babisk *et al.* (2020) obtained clays with flexural strengths of 10–130 kg cm^{-2}. The converted flexural strength of the galette tiles obtained from the Muttalip green clay was greater than these values. Moreover, the flexural strength of the tiles prepared in this work was significantly greater than those obtained from schist materials (156.15 kg cm^{-2}; Kuru Mutlu & Mutlu, 2022). Thus, the material alternatives available to the tile industry can be expanded by developing such clay mixtures, which will reduce the energy costs of industrial processes (Comin *et al.*, 2021).

Absorption and reflection measurements

Absorption and reflection measurements were performed on the galette tiles obtained from Muttalip green clay in three different regions of the electromagnetic spectrum (UV, NIR and MWIR)

https://doi.org/10.1180/clm.2022.38 Published online by Cambridge University Press

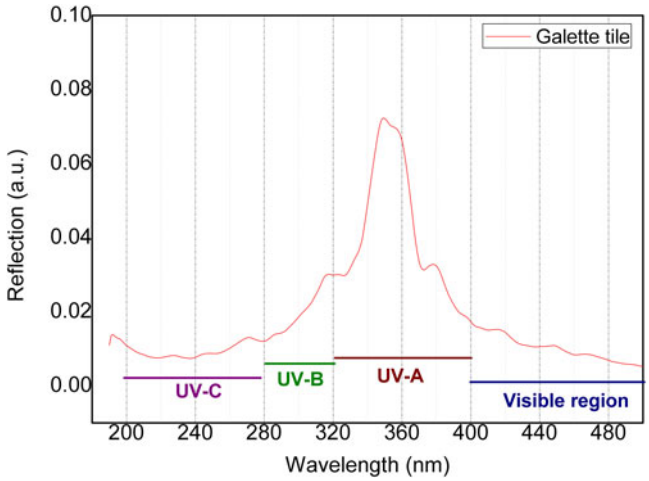

Fig. 6. Reflection spectra of the galette tiles in the UV and visible regions.

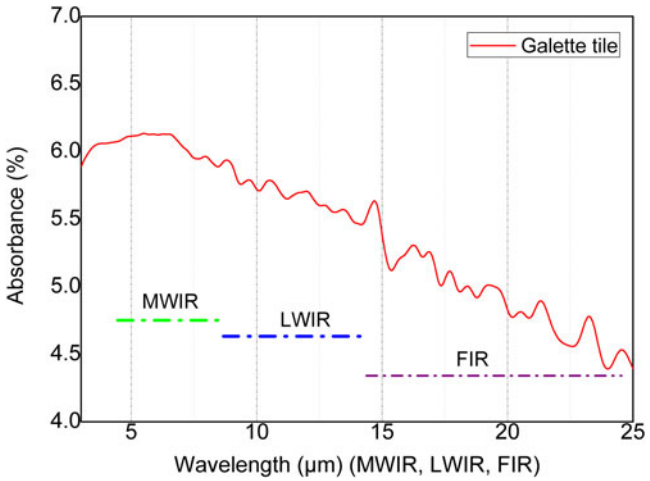

Fig. 8. Absorbance spectra of the galette tiles in the MWIR, LWIR and FIR regions.

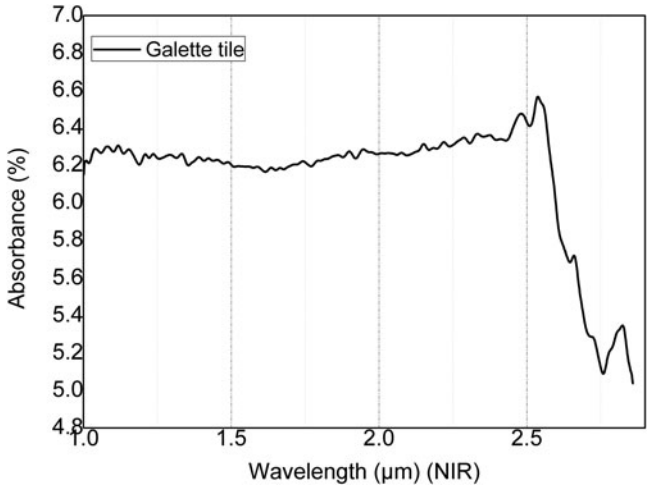

Fig. 7. Absorbance spectra of the galette tiles in the NIR region.

using various detectors, light sources and beam splitters. A vacuum was not required for the absorption–permeability measurements of the tiles in the visible and NIR regions because no atmospheric absorption occurs in these regions. By contrast, because atmospheric absorption occurs in the 2.5–25.0 μm region, optical measurements were performed under vacuum in this region to yield accurate results.

The reflection spectra of the galette tiles (Fig. 6) revealed that their reflection in the UV-B (280–320 nm) region was greater than that in the UV-C (200–280 nm) region. Most UV-B and UV-C rays are absorbed by Earth's atmosphere, and very few of these rays reach Earth's surface. In addition, the amount of light reflected by the tiles in the UV-A region (320–400 nm) was greater than that in the UV-B and UV-C regions (Fig. 6).

Most UV-A radiation from the sun reaches Earth's surface. UV-A exposure causes cell damage in plants (Cavusoglu *et al.*, 2022) and the skin (Radrezza *et al.*, 2021); it also has negative impacts on the eyes (Sherin *et al.*, 2021) and can cause melanoma (Wood *et al.*, 2006; Barnes *et al.*, 2019). However, when UV-A radiation from the sun reached the Muttalip green clay tiles, these tiles reflected the UV-A rays due to their surface properties.

The galette tiles showed consistent absorption in the NIR (1.0–2.5 μm) region (Fig. 7). By contrast, the absorption of the galette tiles in the MWIR region (Fig. 8) decreased as the wavelength increased. Previous studies (Prager *et al.*, 2006; Aboud *et al.*, 2019) have indicated that the ability of tiles to absorb radiation in the IR region is useful for the heating of buildings.

Conclusions

In this study, Muttalip green clay was analysed using XRD, XRF spectroscopy and FE-SEM. The clay was then used to produce tiles with flexural strengths adhering to the TS EN 1304:2016 quality standard. The effect of various firing temperatures (900, 950 and 1000°C) on the flexural strength of the tiles was also investigated. The absorption of the tiles in the MWIR, LWIR and FIR regions of the electromagnetic spectrum was measured under a vacuum to obtain accurate measurement results. Studies on the measurement of such tile absorption under vacuum conditions are limited. Therefore, this study makes an important contribution to the literature.

The flexural strength of tiles prepared from the Muttalip green clay complied with the values listed in the TS EN 1304:2016 standard. The maximum flexural strength of the clay tiles was obtained at a firing temperature of 950°C. In addition, the colour of the tiles darkened with increasing firing temperature.

Muttalip green clay galette tiles reflected significant irradiation in the UV-A region; thus, they offer protection from the harmful effects of UV-A rays. Moreover, the ability of the galette tiles to absorb radiation in the IR region causes heat build-up. The results of the optical characterization experiments conducted in this study detail the advantages of Muttalip green clay and represent another significant contribution to the literature. The Muttalip green clay described in this work can be used as a raw material in the ceramic industry, as tiles made from this clay feature flexural strength that complies with the TS EN 1304:2016 quality standard.

Acknowledgements. The author is grateful to the anonymous reviewers for their constructive comments on this article. The author also thanks the Editor-in-Chief, George Christidis, for his editorial comments and contributions; Hatipoglu Günes Tile & Brick Industry, Inc. in Kutahya, Turkey, for allowing the use of their research and development tile production laboratory;

https://doi.org/10.1180/clm.2022.38 Published online by Cambridge University Press

and Prof. Dr Ugur Serincan at the Eskişehir Nanoboyut Research Laboratory, Eskisehir, Turkey, for enabling the FTIR measurements of the samples.

Financial support. This study did not receive funding from any individual or organization.

Conflicts of interest. The author declares no conflict of interest.

Availability of data and materials. All of the data from this study can be provided upon reasonable request. The analytical equipment, which is regularly checked by the Turkish Standards Institute, was calibrated appropriately. If necessary, samples of the galette tiles can be sent out and shared.

Code availability. No software application or special code was used in this study.

Author contributions. All of the work in this study was conducted by the author.

References

Abdelmalek B., Rekia B., Youcef B., Lakhdar B. & Nathalie F.J.A.C.S. (2017) Mineralogical characterization of Neogene clay areas from the Jijel basin for ceramic purposes (NE Algeria – Africa). 136, 176–183.

Aboud S.A., Altemimi A.B., Al-HiIphy A.R.S., Yi-Chen L. & Cacciola F.J.M. (2019) A comprehensive review on infrared heating applications in food processing. *Molecules*, **24**, 4125.

Ahmed A.N., Sultana M., Zaman M.N. & Rahman M. (2021) Influence of hard rock dust on the physical and microstructural properties of red ceramic materials. *Journal of the Korean Ceramic Society*, **58**, 69–76.

Akçin S.E., Bulut G., Ekinci Şans B. & Esenli F. (2022) The beneficiation of the Pütürge pyrophyllite ore by flotation: mineralogical and chemical evaluation. *Clay Minerals*, doi:10.1180/clm.2022.24.

Assunção A.R.S., Correia G.S., Vasconcelos N.d.S.L., Cabral A.A., Angélica R.S., da Costa F.P. *et al.* (2021) New clayey deposit and their potential as raw material for red or structured ceramics: technological characterization. *Materials*, **14**, 7672.

ASTM C136 (2019) *Standard Test Method for Sieve Analysis of Fine and Course Aggregates*. ASTM International, West Conshohocken, PA, USA, 5 pp.

ASTM C1492 (2003) *Standard Specification for Concrete Roof Tile*. ASTM International, West Conshohocken, PA, USA, 7 pp.

ASTM C830-00 (2016) *Standard Test Methods for Apparent Porosity, Liquid Absorption, Apparent Specific Gravity, and Bulk Density of Refractory Shapes by Vacuum Pressure*. ASTM International, West Conshohocken, PA, USA, 5 pp.

Babisk M.P., Amaral L.F., da Silva Ribeiro L., Vieira C.M.F., do Prado U.S., Gadioli M.C.B. *et al.* (2020) Evaluation and application of sintered red mud and its incorporated clay ceramics as materials for building construction. *Journal of Materials Research Technology*, **9**, 2186–2195.

Barnes G.E. (2013) An apparatus for the determination of the workability and plastic limit of clays. *Applied Clay Science*, **80**, 281–290.

Barnes P.W., Williamson C.E., Lucas R.M., Robinson S.A., Madronich S., Paul N.D. *et al.* (2019) Ozone depletion, ultraviolet radiation, climate change and prospects for a sustainable future. *Nature Sustainability*, **2**, 569–579.

Bilgin N., Bilgin A. & Yeprem H.A. (2008) Isparta killerinden tuğla üretimi. *Afyon Kocatepe Üniversitesi Fen ve Mühendislik Bilimleri Dergisi*, **9**, 203–208.

Bureau of Indian Standards (2002) *Clay Roofing Tiles, Mangalore Pattern – Specification*. Bureau of Indian Standards, Old Dehli, India, 14 pp.

Cavusoglu K., Kalefetoglu Macar T., Macar O., Cavusoglu D. & Yalcın E. (2022) Comparative investigation of toxicity induced by UV-A and UV-C radiation using Allium test. *Environmental Science Pollution Research*, **29**, 33988–33998.

Coletti C., Maritan L., Cultrone G. & Mazzoli C. (2016) Use of industrial ceramic sludge in brick production: effect on aesthetic quality and physical properties. *Construction Building Materials*, **124**, 219–227.

Comin A.B., Zaccaron A., de Souza Nandi V., Inocente J.M., Muller T.G., Dal Bó A.G. *et al.* (2021) Measurement of apparent sintering activation energy for densification of clays. *Clay Minerals*, **56**, 299–305.

Da Costa F.P., Fernandes J.V., de Melo L.R.L., Rodrigues A.M., Menezes R.R. & Neves G.D. (2021) The potential for natural stones from northeastern Brazil to be used in civil construction. *Minerals*, **11**, 440.

De Silva G.H.M.J.S. & Mallwattha M.P.D.P. (2017) Effect of waste rice husk ash on structural, thermal and run-off properties of clay roof tiles. *Construction and Building Materials*, **154**, 251–257.

De Silva G.H.M.J.S. & Mallwattha M.P.D.P. (2018) Strength, durability, thermal and run-off properties of fired clay roof tiles incorporated with ceramic sludge. *Construction Building Materials*, **179**, 390–399.

Guimarães T.C.D.F., Santos A.V.d., Thedoldi A.d.C. & Lima D.C.d. (2022) Study of the physical and mechanical properties with the chemical composition of red clays from the State of Bahia. *Matéria*, **26**, 4.

Huggett J.M. (2015) *Clay Minerals*. Elsevier, Amsterdam, The Netherlands.

Jordán M., Almendro-Candel M., Romero M. & Rincón J.M. (2005) Application of sewage sludge in the manufacturing of ceramic tile bodies. *Applied Clay Science*, **30**, 219–224.

Khoshdast H., Shojaei V., Hassanzadeh A., Niedoba T. & Surowiak A. (2021) A novel open-system method for synthesizing muscovite from a biotite-rich coal tailing. *Minerals*, **11**, 269.

Kuru Mutlu H. (2022) Applied research into Muttalip clay in Eskişehir. *Eskişehir Teknik Üniversitesi Bilim ve Teknoloji Dergisi B – Teorik Bilimler*, **10**, 27–34.

Kuru Mutlu H. & Mutlu A. (2022) Analysis of tiles produced from a schist material and their ultraviolet, near-infrared, mid-infrared, longwave-infrared and far-infrared spectra. *Clay Minerals*, **56**, 292–298.

Lee V.G. & Yeh T.H. (2008) Sintering effects on the development of mechanical properties of fired clay ceramics. *Materials Science and Engineering A – Structural Materials Properties Microstructure and Processing*, **485**, 5–13.

Milheiro F.A.C., Freire M.N., Silva A.G.P. & Holanda J.N.F. (2005) Densification behaviour of a red firing Brazilian kaolinitic clay. *Ceramics International*, **31**, 757–763.

Milošević M., Dabić P., Kovač S., Kaluđerović L. & Logar M.J.C.M. (2019) Mineralogical study of clays from Dobrodo, Serbia, for use in ceramics. *Clay Minerals*, **54**, 369–377.

Milošević M., Logar M. & Djordjević B.J.C.M. (2020) Mineralogical analysis of a clay body from Zlakusa, Serbia, used in the manufacture of traditional pottery. *Clay Minerals*, **55**, 142–149.

Montero M.A., Jordán M., Hernández-Crespo M. & Sanfeliu T. (2009) The use of sewage sludge and marble residues in the manufacture of ceramic tile bodies. *Applied Clay Science*, **46**, 404–408.

Moreno-Maroto J.M., Uceda-Rodríguez M., Cobo-Ceacero C.J., Cotes-Palomino T., Martínez-García C. & Alonso-Azcarate J. (2020) Studying the feasibility of a selection of southern European ceramic clays for the production of lightweight aggregates. *Construction and Building Materials*, **237**, 117583.

Nayak P.S. & Singh B. (2007) Instrumental characterization of clay by XRF, XRD and FTIR. *Bulletin of Materials Science*, **30**, 235–238.

Ofori G. (2019) Construction in developing countries: need for new concepts. *Journal of Construction in Developing Countries*, **23**, 1–6.

Piskin S. & Figen A.K. (2013) Structural characterization of Seydişehir red mud to utilization in roof tile manufacturing. *IFAC Proceedings Volumes*, **46**, 484–487.

Pitarch A., Reig L., Tomás A., Forcada G., Soriano L., Borrachero M. *et al.* (2021) Pozzolanic activity of tiles, bricks and ceramic sanitary-ware in eco-friendly Portland blended cements. *Journal of Cleaner Production*, **279**, 123713.

Prager C., Köhl M., Heck M. & Herkel S. (2006) The influence of the IR reflection of painted facades on the energy balance of a building. *Energy buildings*, **38**, 1369–1379.

Radrezza S., Carini M., Baron G., Aldini G., Negre-Salvayre A. & D'Amato A. (2021) Study of Carnosine's effect on nude mice skin to prevent UV-A damage. *Free Radical Biology Medicine*, **173**, 97–103.

Rivera J.F., Cuarán-Cuarán Z.I., Vanegas-Bonilla N. & de Gutiérrez R.M. (2018) Novel use of waste glass powder: production of geopolymeric tiles. *Advanced Powder Technology*, **29**, 3448–3454.

Sherin P.S., Vyšniauskas A., López-Duarte I., Ogilby P.R. & Kuimova M.K. (2021) Visualising UV-A light-induced damage to plasma membranes of eye lens. *Journal of Photochemistry Photobiology B: Biology*, **225**, 112346.

https://doi.org/10.1180/clm.2022.38 Published online by Cambridge University Press

Simao F.V., Chambart H., Vandemeulebroeke L. & Cappuyns V. (2021) Incorporation of sulphidic mining waste material in ceramic roof tiles and blocks. *Journal of Geochemical Exploration*, **225**, 106741.

Sultana M.S., Ahmed A.N., Zaman M.N., Rahman M.A., Biswas P.K. & Nandy P.K. (2015) Utilization of hard rock dust with red clay to produce roof tiles. *Journal of Asian Ceramic Societies*, **3**, 22–26.

Turkish Republic Prime Ministry State Planning Organization (2008). *9th Development Plan 2007-2013 Specialization Commission Report 1*. Turkish Republic Prime Ministry State Planning Organization, Ankara, Turkey, 127 pp.

Vieira C.M.F., Sanchez R. & Monteiro S.N. (2008) Characteristics of clays and properties of building ceramics in the state of Rio de Janeiro, Brazil. *Construction and Building Materials*, **22**, 781–787.

Wood S.R., Berwick M., Ley R.D., Walter R.B., Setlow R.B. & Timmins G.S. (2006) UV causation of melanoma in *Xiphophorus* is dominated by melanin photosensitized oxidant production. *Proceedings of the National Academy of Sciences of the United States of America*, **103**, 4111–4115.

Yuan J., Yang J., Ma H., Su S., Chang Q. & Komarneni S. (2018) Green synthesis of nano-muscovite and niter from feldspar through accelerated geomimicking process. *Applied Clay Science*, **165**, 71–76.

https://doi.org/10.1180/clm.2022.38 Published online by Cambridge University Press